Sedimentary records of polycyclic aromatic hydrocarbons (PAHs) in remote lakes across the Tibetan Plateau

Ruiqiang Yang[a], Ting Xie[a], An Li[b], Handong Yang[c], Simon Turner[c], Guangjian Wu[d], Chuanyong Jing[a, *]

a: State Key Laboratory of Environmental Chemistry and Ecotoxicology, Research Center for Eco-Environmental Sciences, Chinese Academy of Sciences, P.O. Box 2871, Beijing, 100085, China
b:School of Public Health, University of Illinois at Chicago, Chicago, Illinois 60612, United States
c: Environmental Change Research Centre, University College London, Pearson Building, Gower Street, London WC1E 6BT, U.K.
d: Institute of Tibetan Plateau Research, Chinese Academy of Sciences, Beijing 100101, China

Tel: +86 10 6284 9523; Fax: +86 10 6284 9523
E-mail: cyjing@rcees.ac.cn

ABSTRACT

Sediment cores from five lakes across the Tibetan Plateau were used as natural archives to study the time trends of polycyclic aromatic hydrocarbons (PAHs). The depositional flux of PAHs generally showed an increasing trend from the deeper layers towards the upper layer sediments. The fluxes of PAHs were low with little variability before the 1950s, and then gradually increased to the late 1980s, with a faster increasing rate after the 1990s. This temporal pattern is clearly different compared with those remote lakes across the European mountains when PAHs started to decrease during the period 1960s-1980s. The difference of the temporal trend was attributed to differences in the economic development stages and energy structure between these regions. PAHs are dominated by the lighter 2&3-ring homologues with the averaged percentage over 87%, while it is notable that the percentage of heavier 4-6 ring PAHs generally increased in recent years, which suggests the contribution of local high-temperature combustion sources becoming more predominant.

Capsule:

Increasing contributions from local sources to PAHs in the Tibetan Plateau environment as evidenced from sedimentary records.

Introduction

The Tibetan Plateau (TP) stretches nearly 1,000 km north-to-south and 2,500 km east-to-west in east-central Asia, with the average elevation exceeding 4,500 m. Similar to the polar regions, most parts of the TP are remote and inaccessible, which has led to the presumption of its pristine status. However, the TP is located at low latitude, and surrounded by the rapidly industrializing countries of South and Southeast Asia. Semi-volatile persistent pollutants released from the surrounding source regions can migrate to TP by long-range atmospheric transport (LRAT). In addition, fast growth in population, tourism and gross industral activities in localities within the TP in the past decades may have adversely impacted the environment, altering its previously pristine interior ecosystem.

The lakes on the Plateau differ from lakes in lowlands. The inputs of chemical pollutants to alpine lakes are generally predominated by atmospheric deposition away from direct input (Juttner et al., 1997). Increasingly enhanced global warming in recent decades has accelerated the melting of glacier and frozen soil at high altitude, releasing previously trapped chemical pollutants which may consequently be flushed into alpine lakes (Bogdal et al., 2009). In addition, the post-depositional sediment mixing in deep alpine lakes is relatively limited (Fernandez et al., 2000). The sediments in such lakes are regarded as sentinel indicators of atmospheric pollution due to the lack of local pollution sources (Rose and Rippey 2002; Bettinetti et al., 2011).

62   Polycyclic aromatic hydrocarbons (PAHs) are ubiquitous contaminants. The

63   population growth and industrialization in surrounding areas of the TP have also

64   inevitably increased the releases of PAHs from various combustion processes. The

65   depositional chronology of these chemicals as recorded in relatively undisturbed

66   sediments of alpine lakes in the TP can be used as geochemical markers of economic

67   and social development impacts (Han et al., 2015). Yang et al. (2010) reconstructed

68   mercury pollution using lake sediments from the TP. Cheng et al. (2014) reported time

69   trends of OCP pollution by analyzing sediments from three lakes in the central TP.

70   Wang et al. (2010) and Han et al. (2015) reconstructed PAH pollution in Lake Qinghai

71   of the northern TP. These studies documented that sediment of the TP could archive

72   important environmental information about past anthropogenic influence. However,

73   the sedimentary PAH data across the TP, especially in the southern and central TP is

74   so far very limited.

75   The basic hypotheses of the present study are that sediment contamination of

76   lakes in the TP is associated with the industrialization and human activities of major

77   Asian countries, and that over the past three decades, the rapid economic development

78   and population growth within the TP have contributed to the overall burden of

79   pollutants in the environment. In this study, a total of 157 samples from five sediment

80   cores were analyzed for PAHs. The objectives were to reveal the spatial patterns along

81   a southwest-to-northeast transect across TP, reconstruct the deposition history, and

82   gain insights on sources of the PAHs in the sediments.

1. Materials and methods

1.1. Study Area and Sampling

Five lakes were selected across a southwest-to-northeast transect: Peiku Co, Nam Co,

Cuo E, Cuo Na and Keluke Lake (Fig. 1). All the lakes are remote and far from urban

or agricultural pollution sources and are covered annually with ice for at least several

months. All the studied lakes are freshwater except for Cuo E, which is brackish with

salinity of 892 mg/L in Cl^- (Lami et al. 2010). Keluke is a closed basin in the

semi-arid, grassland-steppe climate zones in the northeast TP with no river flowing in

or out of the lake. Nam Co and Peiku Co lakes have glaciers in their catchments

(Lami et al. 2010). Peiku Co is a typical tectonic lake caused by the uplift of

Himalayan Mountains at the southern edge of the TP, and precipitation as well as

glacier melt water is the main water supply (Nie et al., 2013). The latitude, longitude,

and altitude of the lakes as well as the surface areas and depths are given in Table 1.

Sediment cores were collected in August 2006 and 2007. A HTH gravity corer

with an 8.5 cm inner diameter polycarbonate tube was used to collect sediment cores

at adjacent locations within 3 meters of each other in each lake. Cores were collected

from the deepest part of the lakes, except the two from Nam Co and Peiku Co, where

they were taken from the shallower sub-basins. One core from each site was assigned

for organic pollutants analyses in this study. The length of the cores ranged from 24 to

43 cm (Table 1). The core was sectioned onsite at intervals of 0.5 cm using a stainless

steel cutter. All samples were packed in aluminum foil and were stored at 4°C in a car

104 refrigerator during transportation, and then they were kept frozen at -20°C in the

105 laboratory.

1.2. Sediment Characterization

107 The samples were analyzed for water content and wet bulk density, from which the

108 porosity and dry bulk density were calculated. Organic matter (OM) content of each

109 section was determined gravimetrically by loss on ignition (LOI) at 550°C for 4 h.

110   A sediment core from each lake was analyzed for ^{210}Pb, ^{226}Ra, ^{137}Cs and ^{241}Am

111 by direct measuring radioactivity using γ-ray spectroscopy in the Environmental

112 Radiometric Facility at University College London, using an ORTEC HP Ge GWL

113 series well-type coaxial low background intrinsic germanium detector. The detailed

114 radiometric dating method is described in the previous work (Yang et al., 2010).

115 Sediment ages and mass sedimentation rates (MSR) were calculated using constant

116 rate of supply (CRS) model. The sediment focusing factor (FF), which was needed to

117 evaluate the post-depositional horizontal movement of the sediment particles, was

118 calculated as the ratio of the unsupported ^{210}Pb inventory in the sediments in the

119 coring location to that expected from the regional atmospheric input (Yang et al., 2010)

120 and the results are included in Table 1.

1.3. Chemical Analysis

122 A PAH mixture standard, a surrogate mixture standard, and the internal standard

123 2-fluorobiphenyl were purchased from Accustandard (New Haven, CT). The PAH

124 mixture standard contained 16 individual compounds including naphthalene (NAP),

125 acenaphthylene (ACY), acenaphthene (ACP), fluorene (FLR), phenanthrene (PHE),

126 anthracene (ANT), fluoranthene (FLT), pyrene (PYR), benz[a]anthracene (BaA),

127 chrysene (CHR), benz[b]fluoranthene (BbF), benz[k]fluoranthene (BkF),

128 benz[a]pyrene (BaP), indeno[1,2,3-cd]pyrene (IcdP), dibenzo[a,h]anthracene (DahA),

129 and benzo[ghi]perylene(BghiP). The surrogate mixture standard had five deuterated

130 PAHs including naphthalene-d8 (NAP-d8), acenaphthene-d10 (ACP-d10),

131 phenanthrene-d10 (PHE-d10), chrysene-d12 (CHR-d12) and perylene-d12 (PER-d12).

132 The solvents n-hexane and dichloromethane used for extraction and cleanup

133 were ultra residue-analytical grade and were purchased from Fisher Scientific

134 (Andover, USA). Alumina (100-200 mesh, Sigma-Aldrich, USA) and Silica gel

135 (100-200 mesh, Qingdao Marine Chemical, China) were baked at 550°C for 12 hrs

136 and activated at 180°C for 2 hrs. Anhydrous sodium sulfate was baked at 550°C for 4

137 hrs. Copper powder (200 mesh, Sinopharm Chemical Reagent Co. Ltd, China) was

138 activated before use.

139 Freeze-dried and ground sediment samples (1 g) were spiked with surrogates and

140 extracted using mixed solvents of hexane and dichloromethane (DCM) (1:1, v/v) by

141 accelerated solvent extraction (Dionex ASE350, U.S.) at a temperature of 150°C and a

142 pressure of 1500 psi. Activated copper powder was added to the extract to remove

143 elemental sulfur. The extracts were concentrated to about 1~2 ml by a rotary

144 evaporator. The cleanup was conducted using a glass column packed with 6 g 3%

145 deactivated silica gel, 4 g 2% deactivated alumina and 2-cm-thickness of anhydrous

146 sodium sulfate from bottom to top. The elution was subsequently conducted using 10

147 ml of hexane and a 50 ml mixture of dichloromethane and hexane (1:1, v/v). The

148 effluent was concentrated to 0.5 ml. Quantitative internal standard (200 ng of

149 4,4'-difluorobiphenyl) were finally added to the extract before instrumental analysis.

150 An Agilent-7890 gas chromatograph (GC) equipped with an HP-5 MS capillary

151 column (30 m×0.25 mm i.d. ×0.25 um film thickness) was used to separate PAHs

152 while a mass spectrometer (MS, Agilent 5975) with electron ionization (EI) was used

153 to analyze PAHs. The oven temperature program was operated as follows: initial 60°C

154 for 2 min, 6°C /min to 300°C, and held for a final 10 min. The temperature of the

155 injector was set at 280°C. High-purity helium was used as the carrier gas with a

156 constant flow of 1 ml/min. The MS detector was operated at 70 eV and the ion source

157 was set at 300°C. The quadrupole and interface temperatures were 180°C and 300°C,

158 respectively. The MS detector was operated in selected ion monitoring (SIM) mode.

159 **1.4. Quality Control**

160 A procedural blank using Na_2SO_4 in place of sediment was analyzed in each batch of

161 11 sediment samples. Only trace levels of targets were detected in blanks, and were

162 subtracted from those in sediment samples. The average recoveries of spiked

163 surrogates in all analyzed samples (N=157) were 70-136% for the five deuterated

164 PAHs. The concentrations reported in this paper were corrected by the surrogate

165 recoveries. One or two segments in each core were analyzed in duplicate, and the

166 average relative percentage differences (RPDs) were in the range of 5.1-31.1%. The

167 method detection limit (MDL) was defined as 3:1 signal-to-noise ratio (S/N) and

168 ranged 0.01-0.41 ng/g dw. The instrument performance was routinely checked using

169   quality control standards.

1.5. Estimation of Chemical Flux

171   Flux stands for the accumulation rate of the chemical analyte. Since concentration

172   may be strongly affected by dilution of detrital matter and water content, flux has

173   been considered as a more meaningful way to assess pollutant inputs than

174   concentration (Elmquist et al., 2007). The flux was estimated by the following

175   equation:

176
$$\text{Flux}_i\,(\mu g/m^2/yr) = C_i \times MSR \times 10/FF$$

177   where C_i is the dry-weight-based concentration in sediment core segment i (ng/g dw),

178   MSR is mass sedimentation rate (g/cm^2/yr), FF is the focusing factor(dimensionless),

179   reflecting the post-depositional horizontal movement of sediment particles on the lake

180   bottom due to turbulence. The FF value was calculated as the ratio of unsupported

181   ^{210}Pb accumulation in a core to that atmospheric ^{210}Pb deposition flux in lake basin

182   soil. Detailed information was described by Yang et al., (2010).

2. Results and discussion

2.1. Concentrations

185   The concentrations of total PAHs (Σ_{16}PAH) in the sediment cores of the five lakes

186   ranged from 98-595 ng/g. The Σ_{16}PAH concentration profiles in the cores varied

187   among lakes (Fig. 2A). The PAH concentrations in this study were compared with

those sediments from other remote lakes (Table 2). The PAH concentrations were generally higher than those reported previously for sediments from the Arctic (27-140 ng/g, Σ_{15}PAH excluding benz(a)anthracene) (Jiao et al., 2009), the Antarctic (1.4-205 ng/g) (Klanova et al., 2008) and Rocky Mountains (31-280 ng/g) (Usenko et al., 2007). The average Σ_{15}PAH (176 ng/g, excluding naphthalene) in the sediments of this study was approximately double that from the southern slope of the Himalayas in Nepal (68 ± 22 ng/g) (Guzzella et al., 2011). The PAH concentrations in this study were in the same order of magnitude with those reported in sediment from the Andes mountains (32-862 ng/g) (Barra et al., 2006) but 1~2 orders of magnitude lower than those in sediments from European mountains (Rose and Rippey 2002; van Drooge et al. 2011). The elevated concentrations in the TP might be due to its proximity to possible source regions. The lakes in this study, especially in the southern and central areas, are located at altitude over 4500 m a.s.l. and are likely to be in the free troposphere. Deposited PAHs at these altitudes is likely to be derived from LRAT sources, most probably from Indian subcontinent and China inland areas. Precipitation on the TP is strongly controlled by the Asian monsoon system (Pant et al., 1997). Studies have documented that the transport and fate of contaminants to TP are likely to be significantly influenced by regional monsoon systems (Yang et al., 2008; Wang et al., 2008; Yang et al., 2010).

The 16 PAHs were grouped into 2&3-rings (NAP, ACY, ACP, FLR, PHE and ANT), 4-ring (FLT, PYR, BaA and CHR) and 5&6-rings (BbF, BkF, BaP, IcdP, DahA, and BghiP). Because high molecular weight PAHs are mostly generated from high

210   temperature combustion, such as in coke ovens and diesel engines (Mai et al., 2003),

211   the sum of the 5 and 6-ring PAHs Σ_7PAH (BaA, CHR, BbF, BkF, BaP, IcdP and DahA)

212   is a good indicator in reflecting the impacts of industrial and traffic emissions. In this

213   study, the increasing trends of Σ_7PAH are even clearer than Σ_{16}PAH in all studied

214   lakes (Fig. 2B). Therefore, the Σ_7PAH can be a more appropriate parameter to reflect

215   the anthropologic impacts by human activities on the TP.

216   **2.2. Deposition flux and historical trends**

217   Differing with concentration profiles in cores, fluxes calculated by considering

218   variation in sedimentation rate, show a general increasing trend from the deeper layers

219   towards the upper layer sediments (Fig. 2). The PAH fluxes were low with little

220   variability before the 1950s, and then gradually increased from the 1950s to the late

221   1980s, and the increase appears to have accelerated from the 1990s. This temporal

222   pattern is clearly different from those found in remote mountain lakes across Europe,

223   where the pyrolytic PAHs peaked in the 1960s-1980s (Fernandez et al., 2000). The

224   period (from the 1960s to the 1980s) during which PAHs started to decrease in the

225   developed countries is when PAH emissions started to increase rapidly in the

226   surroundings of the TP, as observed in the present study. The difference of the

227   temporal trend was attributed to differences in the economic development stages and

228   energy structure between the early industrialized and newly industrialized countries.

229   Nevertheless, the vertical profile of PAH flux is somewhat different among

230   individual lakes. The temporal resolution of Peiku Co is relatively poor due to its low

231 sedimentation rate; but on the other hand, this allows observing a temporal trend of

232 accumulation covering more than 200 yrs. In addition, it is notable that temporal

233 profile in Nam Co seems relatively stable since 1950 until post-2000, differing with

234 other studied lakes (Fig. 2). The Nam Co Core was taken in a bay in the southeast of

235 the lake and un-decomposed algal gel appeared above ca. 20 cm (Fig. S1). The

236 abundance of the algae increased significantly upwards to the sediment surface

237 (organic matter content from 14.7% at 20 cm to 27.4% in the surface). Correlation

238 analysis between $\Sigma_{16}PAH$ concentration and organic matter content showed

239 significantly negative correlation (correlation coefficient R = -0.593, P=0.012),

240 indicating the possible dilution role of algae on PAH concentrations in sediment,

241 which was also confirmed by Yang et al (2010) that mercury concentration was

242 diluted by algae in Nam Co Lake. Differences between these sites may be attribute to

243 the locations of lakes of the plateau with different meteorological conditions and

244 proximity to sources.

245 **Implications for Sources**

246 Fig. 3 clearly shows that the low molecular weight PAHs (2-3 rings) are dominant in

247 the sediments of the TP with an average percentage over 87%. This is considerably

248 different from the patterns in source regions of the South China Sea (Liu et al., 2012)

249 where high molecular weight PAHs dominate. The lighter PAHs are more easily

250 transported to the remote TP through LRAT, which might be an explanation to the

251 dominance of low molecular weight PAHs (Tao et al., 2011; Yang et al., 2013). In

252 addition, biomass burning, which is commonly used heating source in the TP,

253 produces more lighter PAHs. In contrast to this, within more developed regions,

254 industrial and traffic related combustion emits higher proportions of heavier PAHs

255 (Bhatt and Sachan, 2004).

256 Temporal variations in PAH compositions have been used as an indicator of a

257 shift in PAH sources (Liu et al., 2012a). The percentage of heavier PAHs (4-6 rings)

258 increased in recent years in most of the lakes of this work (Fig. 3). In particular, the

259 fractions of 5-ring BbF, which is a known product of high-temperature combustion

260 (Mai et al., 2003), and 6-ring IcdP and BghiP, which are tracers of vehicle exhaust

261 (Harrison et al. 1996), have increased 2.0 and 3.5 fold, respectively, since the year

262 1990 in Cuo Na lake (Fig. 4A). The concentration profiles show similarly increasing

263 trends with fluxes (Fig. S2). These observations suggest the increasing contribution of

264 local, high-temperature combustion sources in the past decade, when Tibet has

265 experienced exponential growths in population, tourism, and gross industrial activities

266 (Fig. 4B). The remarkable increase of IcdP and BghiP concentrations (tracers of

267 vehicle exhaust) in Cuo Na Lake possibly resulting from the rapid increasing

268 emissions by traffic and transportation in recent years due to its relatively close to the

269 Qinghai-Tibet highway and Qinghai-Tibet Railway. The variation of PAH pattern in

270 sediment is an evidence that the rapid social economical changes in Tibet have

271 impacted its previously pristine ecosystem. These concerns have been raised from

272 other studies (Wang et al., 2010; Yang et al., 2010; Cong et al., 2013).

273   Diagnostic concentration fractions of PAH isomers, such as ANT/(ANT+PHE),

274   BaA/(BaA+CHR), FLT/(FLT+PYR) and IcdP/(IcdP+BghiP) are often applied for

275   source identification purposes (Yunker et al., 2002; Liu et al., 2012b). ANT and BaA

276   are believed to be more susceptible to photochemical degradation than their isomers

277   (Behymer and Hites 1988; Zhang et al., 2005; Liu et al., 2012b). However, the

278   FLT/PYR and IcdP/BghiP isomer pairs were diluted and degraded at analogous rates,

279   so the ratios of FLT/(FLT+PYR) and IcdP/(IcdP+BghiP) might be more suitable for

280   defining sources of PAHs in remote areas like TP. In this study, most of the measured

281   ratios of IcdP/(IcdP+BghiP) and FLT/(FLT+PYR) were greater than 0.2 and 0.4,

282   respectively (Fig. 5). According to the source classification by Yunker et al. (2002),

283   the sources of PAHs in the sediments are mainly from grass, biomass & coal

284   combustion. The vertical patterns of the investigated congeners were relatively

285   consistent and without any general trends throughout the whole length of the cores,

286   apart from the decrease in the ratios of IcdP/(IcdP+BghiP) in the superficial segments

287   of Cuo Na Lake (Fig. S3).

288   **3. Conclusion**

289   In this study, five sediment cores across the TP were analysed for PAHs with the

290   objective examining their time trends. The depositional flux of PAHs generally

291   showed an increasing trend from the deeper layers towards the upper layer sediments,

292   with a faster increasing rate after the 1990s, which were apparently different from

293   those reported in European mountains. The dominant of lighter PAHs indicates they

294   are mainly from grass, biomass & coal combustion and/or from LRAT. Particular

295   concern is the recent shift in PAH sources. The percentage of heavier PAH (4-6 rings)

296   increased rapidly in the past two decades suggest increasing contribution of local,

297   high-temperature combustion sources in the TP.

303   **Appendix. Supplementary data**

304   Supplementary data associated with this article can be found in the online version.

References

Barra, R., Popp, P., Quiroz, R., Treutler, H. C., Araneda, A., Bauer, C., Urrutia, R., 2006. Polycyclic aromatic hydrocarbons fluxes during the past 50 years observed in dated sediment cores from Andean mountain lakes in central south Chile. Ecotox. Environ. Safe. 63, 52-60.

Behymer, T. D., Hites, R. A., 1988. Photolysis of polycyclic aromatic hydrocarbons adsorbed on fly ash. Environ. Sci. Technol. 22, 1311-1319.

Bettinetti, R., S., Galassi, S., Guilizzoni, P., Quadroni, S., 2011. Sediment analysis to support the recent glacial origin of DDT pollution in Lake Iseo (Northern Italy). Chemosphere. 85, 163-169.

Bhatt, B. P., Sachan, M. S., 2004. Firewood consumption along an altitudinal gradient in mountain villages of India. Biomass Bioenergy. 27, 69-75.

Bogdal, C., P., Schmid, P., Kohler, M., Muller, C. E., Iozza, S., Bucheli, T. D., Scheringer, M., Hungerbuhler, K., 2009. Blast from the past: melting glaciers as a relevant source for persistent organic pollutants. Environ. Sci. Technol. 43, 8173-8177.

Cheng, H. R., Lin, T., Zhang, G., Liu, G. Q., Zhang, W. L., Qi, S. H., Jones, K. C., Zhang, X. W., 2014. DDTs and HCHs in sediment cores from the Tibetan Plateau. Chemosphere 94, 183-189.

Cong, Z. Y., Kang, S. C., Gao, S. P., Zhang, Y. L., Li, Q., Kawamura, K., 2013. Historical trends of atmospheric black carbon on Tibetan Plateau as reconstructed from a 150-year lake sediment record. Environ. Sci. Technol. 47, 2579-2586.

Elmquist, M., Zencak, Z., Gustafsson, Ö., 2007. A 700 year sediment record of black carbon and polycyclic aromatic hydrocarbons near the EMEP air monitoring station in Aspvreten, Sweden. Environ. Sci. Technol. 41, 6926-6932.

Fernandez, P., Vilanova, R. M., Martinez, C., Appleby, P., Grimalt, J. O., 2000. The historical record of atmospheric pyrolytic pollution over Europe registered in the sedimentary PAH from remote mountain lakes. Environ. Sci. Technol. 34 1906-1913.

Guzzella, L., Poma, G., De Paolis, A., Roscioli, C., Viviano, G., 2011. Organic persistent toxic substances in soils, waters and sediments along an altitudinal gradient at Mt. Sagarmatha, Himalayas, Nepal. Environ. Pollut. 159, 2552-2564.

Han, Y. M., Wei, C., Bandowe, B. A. M., Wilcke, W., Cao, J. J., Xu, B. Q., Gao, S. P., Tie, X. X., Li, G. H., Jin, Z. D., An, Z. S., 2015. Elemental carbon and polycyclic aromatic compounds in a 150-year sediment core from Lake Qinghai, Tibetan Plateau, China: influence of regional and local sources and transport pathways. Environ. Sci. Technol. 49, 4176-4183.

Harrison, R. M., Smith, D. J., T. Luhana, L., 1996. Source apportionment of atmospheric polycyclic aromatic hydrocarbons collected from an urban location in Birmingham, UK. Environ. Sci. Technol. 30, 825-832.

Jiao, L. P., G. J. Zheng, G. J., Minh, T. B., Richardson, B., Chen, L. Q., Zhang, Y. H., Yeung, L. W.,

Lam, J. C. W., Yang, X. L., Lam, P. K. S., Wong, M. H., 2009. Persistent toxic substances in remote lake and coastal sediments from Svalbard, Norwegian Arctic: Levels, sources and fluxes. Environ. Pollut. 157, 1342-1351.

Juttner, I., B., Henkelmann, B., Schramm, K. W., Steinberg, C. E. W., Winkler, R., Kettrup, A., 1997. Occurrence of PCDD/F in dated lake sediments of the Black Forest, southwestern Germany. Environ. Sci. Technol. 31, 806-812.

Klanova, J., N., Matykiewiczova, N., Macka, Z., Prosek, P., Laska, K., Klan, P., 2008. Persistent organic pollutants in soils and sediments from James ROSS Island, Antarctica. Environ. Pollut. 152, 416-423.

Lami, A., Turner, S., Musazzi, S., Gerli, S., Guilizzoni, P., Rose, N. L., Yang, H. D., Wu, G. J., Yang, R. Q., 2010. Sedimentary evidence for recent increases in production in Tibetan plateau lakes. Hydrobiologia 648, 175-187.

Liu, L.Y., Wang, J. Z., Wei, G. L., Guan, Y. F., Wong, C. S., Zeng, E. Y., 2012a. Sediment records of polycyclic aromatic hydrocarbons (PAHs) in the continental shelf of China: implications for evolving anthropogenic impacts. Environ. Sci. Technol. 46, 6497-6504.

Liu, L. Y., Wang, J. Z., Wei, G. L., Guan, Y. F., Zeng, E. Y., 2012b. Polycyclic aromatic hydrocarbons (PAHs) in continental shelf sediment of China: implications for anthropogenic influences on coastal marine environment. Environ. Pollut. 167, 155-162.

Mai, B. X., Qi, S. H., Zeng, E. Y., Yang, Q. S., Zhang, G., Fu, J. M., Sheng, G. Y., Peng, P. N., Wang, Z. S., 2003. Distribution of polycyclic aromatic hydrocarbons in the coastal region off Macao, China: Assessment of input sources and transport pathways using compositional analysis. Environ. Sci. Technol. 37, 4855-4863.

NBSC. China Statistical Yearbook 1949-2008; China Statistics Press, Beijing.

Nie, Y., Zhang, Y. L., Ding, M. J., Liu, L. S., Wang, Z. F., 2013. Lake change and its implication in the vicinity of Mt. Qomolangma (Everest), central high Himalayas, 1970-2009. Environ. Earth Sci. 68, 251-265.

Pant, G.B., Rupa, Kumar, K., 1997. Climates of South Asia. John Wiley and Sons, Chichester.

Rose, N. L., Rippey, B., 2002. The historical record of PAH, PCB, trace metal and fly-ash particle deposition at a remote lake in north-west Scotland. Environ. Pollut. 117, 121-132.

Tao, S., Wang, W. T., Liu, W. X., Zuo, Q. A., Wang, X. L., Wang, R., Wang, B., Shen, G. F., Yang, Y. H., He, J. S., 2011. Polycyclic aromatic hydrocarbons and organochlorine pesticides in surface soils from the Qinghai-Tibetan plateau. J. Environ. Monitor. 13, 175-181.

Usenko, S., Landers, D. H., Appleby, P. G., Simonich, S. L., 2007. Current and historical deposition of PBDEs, pesticides, PCBs, and PAHs to rocky mountain national park. Environ. Sci. Technol.41, 7235-7241.

van Drooge, B. L., Lopez, J., Fernandez, P., Grimalt, J. O., Stuchlik, E., 2011. Polycyclic aromatic hydrocarbons in lake sediments from the High Tatras. Environ. Pollut. 159, 1234-1240.

Wang, X. P., Xu, B. Q., Kang, S. C., Cong, Z. Y., Yao, T. D., 2008. The historical residue trends of DDT, hexachlorocyclohexanes and polycyclic aromatic hydrocarbons in an ice core from Mt. Everest, central Himalayas, China. Atmos. Environ. 42, 6699-6709.

Wang, X. P., Yang, H. D., Gong, P., Zhao, X., Wu, G. J., Turner, S., Yao, T. D., 2010. One century sedimentary records of polycyclic aromatic hydrocarbons, mercury and trace elements in the Qinghai Lake, Tibetan Plateau. Environ. Pollut. 158, 3065-3070.

Xiang, J., Zheng, M.P., 1989. Saline Lakes on the Qinghai-Tibet Plateau. Beijing Science & Technology Press, Beijing.

Yang, H., Battarbee, R. W., Turner, S. D., Rose, N. L., Derwent, R. G., Wu, G. J., Yang, R. Q., 2010. Historical reconstruction of mercury pollution across the Tibetan Plateau using lake sediments. Environ. Sci. Technol. 44, 2918-2924.

Yang, R.Q., Yao, T.D., Xu, B.Q., Jiang, G.B., Zheng, X.Y., 2008. Distribution of organochlorine pesticides (OCPs) in conifer needles in the southeast Tibetan Plateau. Environ. Pollut. 153, 92-100.

Yang, R. Q., Zhang, S. J., Li, A., Jiang, G. B., Jing, C. Y., 2013. Altitudinal and spatial signature of persistent organic pollutants in soil, lichen, conifer needles, and bark of the southeast Tibetan Plateau: implications for sources and environmental cycling. Environ. Sci. Technol. 47, 12736-12743.

Yunker, M. B., Macdonald, R. W., Vingarzan, R., Mitchell, R. H., Goyette, D., Sylvestre, S., 2002. PAHs in the Fraser River basin: a critical appraisal of PAH ratios as indicators of PAH source and composition. Org. Geochem. 33, 489-515.

Zhang, X., Tao, S., Liu, W. X., Yang, Y., Zuo, Q., Liu, S. Z., 2005. Source diagnostics of polycyclic aromatic hydrocarbons based on species ratios: a multimedia approach. Environ. Sci. Technol. 39, 9109-9114.

Table 1. Lake characteristics, geographic coordinates and focusing factor (FF) in the studied lakes.

Lakes	Latitude (N)	Longitude (E)	Lake Altitude (m)	Lake Area [a] (km^2)	Salinity [b] (Cl$^-$ mg/L)	Core length (cm)	Core water depth (m)	Focusing Factor [c]
Keluke	37°17.165′	96°52.922′	2813	57	fresh(116.5)	25.0	8.3	0.72
Cuo Na	32°02.921′	91°30.805′	4617	182	fresh(8.98)	43.0	12.4	5.97
Cuo E	31°25.221′	91°29.087′	4531	61	brackish(892)	29.5	8.4	6.26
Nam Co	30°46.203′	90°55.715′	4630	1982	fresh(166)	42.0	21.6	1.58
Peiku Co	28°48.726′	85°31.015′	4595	284	fresh(103)	24.5	16.3	0.17

[a:] (Xiang and Zheng, 1989); [b:] (Lami et al., 2010); [c:] (Yang et al., 2010).

**Table 2** Comparison of PAH concentrations (ng/g dw) in sediments from remote lakes.

| Location	Sampling year	Sediment type	Concentration	No. of congener[a]	Reference
Mountain lakes, across TP	2006-07	core	98-594	$\sum_{16}$PAH [b]	This study
Qinhai Lake, northern TP	2006	core	11-279	$\sum_{15}$PAH[c]	(Wang et al., 2010)
Southern Himalaya lakes, Nepal	2007	surface	68 ±22	$\sum_{15}$PAH[c]	(Guzzella et al., 2011)
Andean mountain lakes, Chile	2002	core	32-862	$\sum_{16}$PAH	(Barra et al., 2006)
High Tatras, Eastern Europe	2001	surface	1800-30000	$\sum_{15}$PAH[d]	(van Drooge et al., 2011)
Remote lake, north-west Scotland	1996	core	626-1719	$\sum_{16}$PAH	(Rose and Rippey, 2002)
Rocky Mountain, North America	2003	core	31-280	$\sum_{16}$PAH	(Usenko et al., 2007)
Ny-Alesund lakes, Norway Arctic	2005	surface	27-140	$\sum_{15}$PAH[e]	(Jiao et al., 2009)
James Ross Island, Anarctic	2005	surface	1.4-205	$\sum_{16}$PAH	(Klanova et al., 2008)

[a]: The PAH levels selected for comparison were chosen from the studies having similar compound groupings; [b]: sum of 16 US EPA priority PAHs; [c]: 16 US EPA PAHs excluding naphthalene; [d]: 16 US EPA PAHs excluding naphthalene, acenaphthene and acenaphthylene plus perylene and benzo(e)pyrene; [e]: 16 US EPA PAHs excluding benza(a)anthracene.

Figure legends:

Figure 1   Map showing locations of the lakes cored for this study.

Figure 2   Temporal trends of concentrations (blue diamond) and depositional fluxes (red circle) for Σ_{16}PAH (A) and Σ_7PAH (B) in dated sediment cores of the Tibetan Plateau.

Figure 3   Relative percentage of PAHs against deposition year in lake sediments. 2&3-ring (NAP, ACY, ACP, FLR, PHE and ANT), 4-ring (FLT, PYR, BaA and CHR) and 5&6-ring (BbF, BkF, BaP, IcdP, DahA and BghiP).

Figure 4   Deposition fluxes of selected PAHs in Lake Cuo Na (A) and population and economic development data of Tibet* (B). *Data from NBSC. China Statistical Yearbook 1949-2008; China Statistics Press, Beijing.

Figure 5   Bivariate plot of PAH diagnostic ratios in lake sediments.
PAH sources identification by Yunker et al., (2002): FLT/(FLT+PYR) < 0.4: petroleum, 0.4 < FLT/(FLT+PYR) < 0.5: petroleum combustion, FLT/(FLT+PYR) > 0.5: grass, wood and coal combustion; IcdP/(IcdP+BghiP) < 0.2: petroleum, 0.2 <IcdP/(IcdP+BghiP) < 0.5: petroleum combustion, IcdP/(IcdP+BghiP) > 0.5: grass, wood and coal combustion.
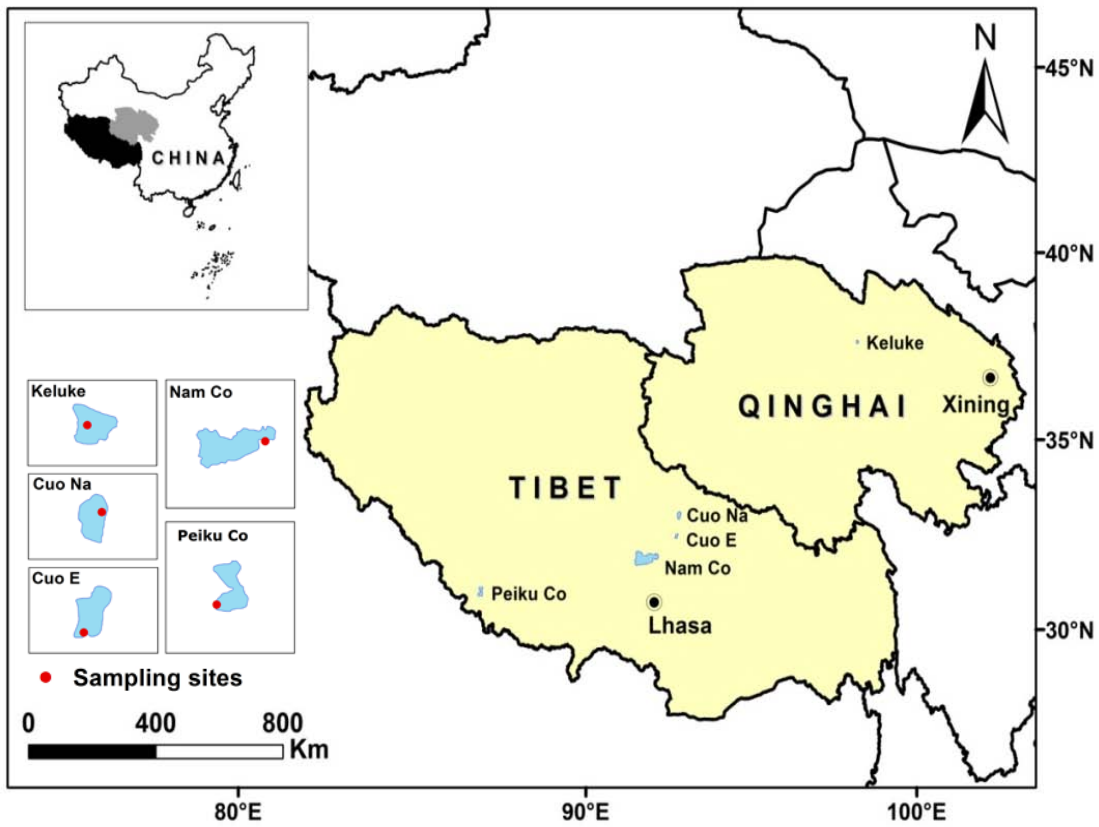
Fig. 1 Map showing location of the lakes cored for this study.
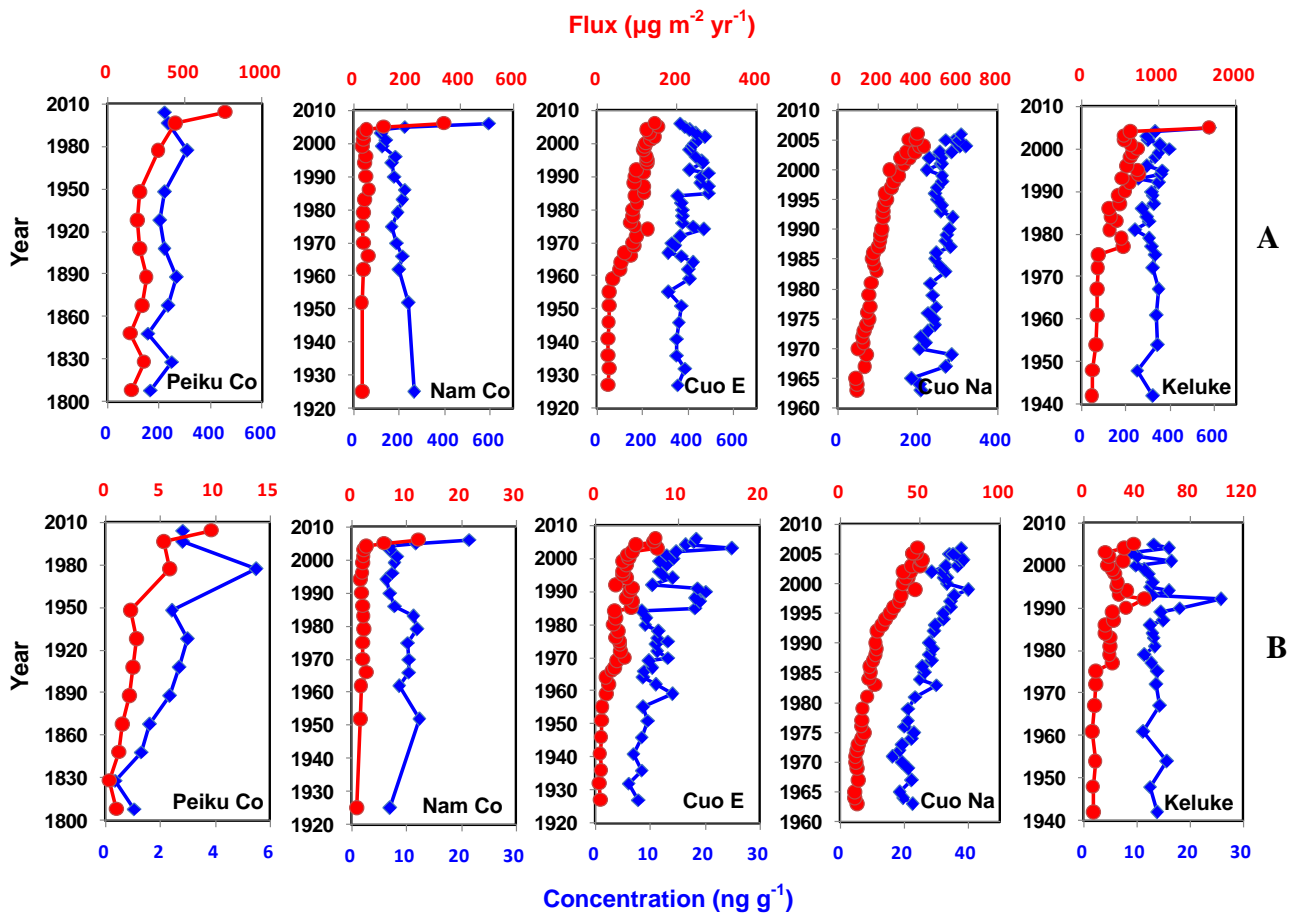
Fig.2 Temporal trends of concentrations (blue diamond) and depositional fluxes (red circle) for Σ_{16}PAH (A) and Σ_7PAH (B) in dated sediment cores of the Tibetan Plateau.
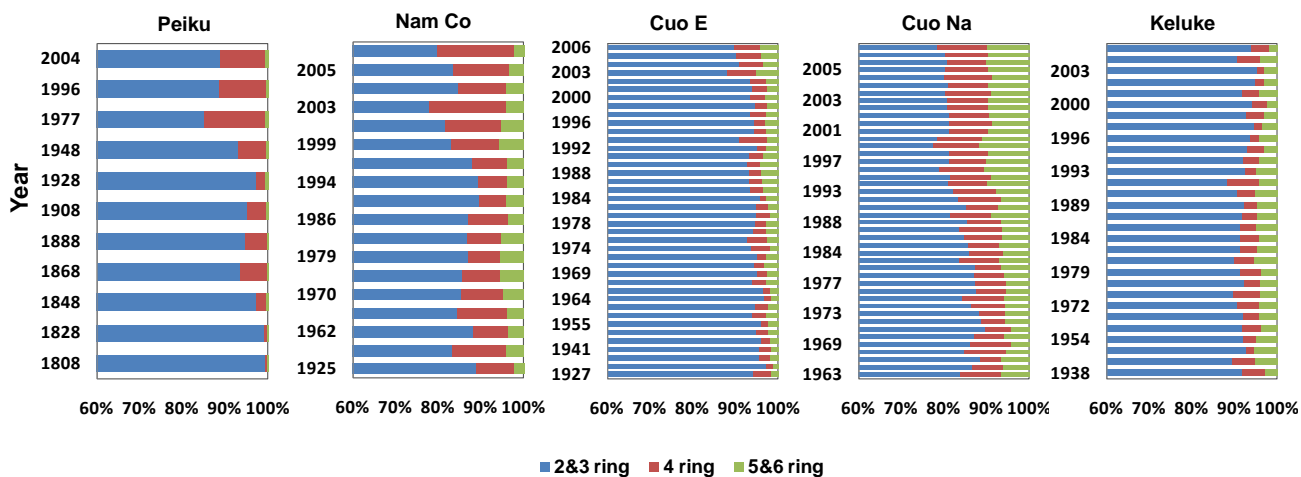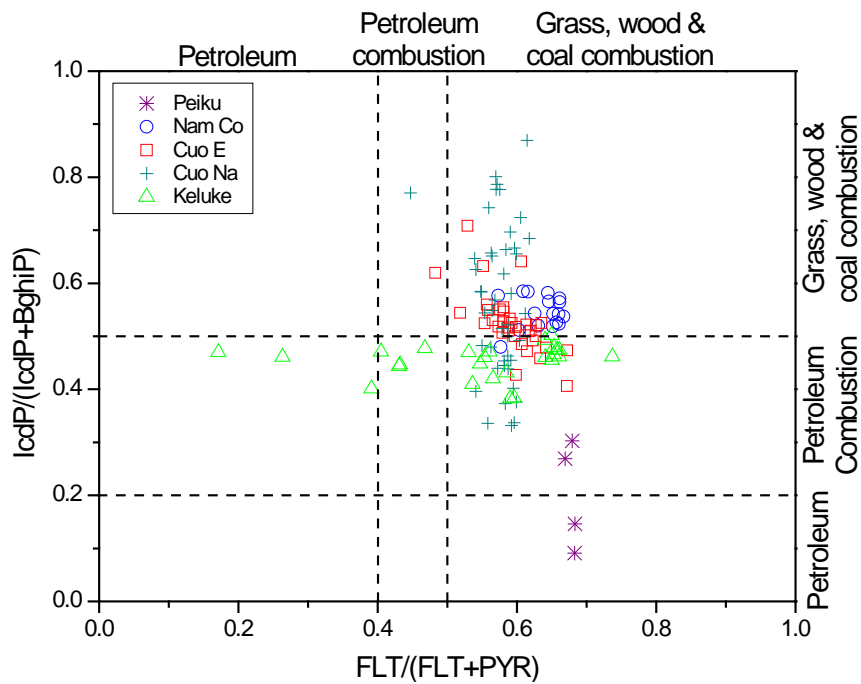
Fig. 3 Relative percentage of grouped PAHs against deposition year in lake sediments. 2&3-ring (NAP, ACY, ACP, FLR, PHE and ANT), 4-ring (FLT, PYR, BaA and CHR) and 5&6-ring (BbF, BkF, BaP, IcdP, DahA and BghiP).
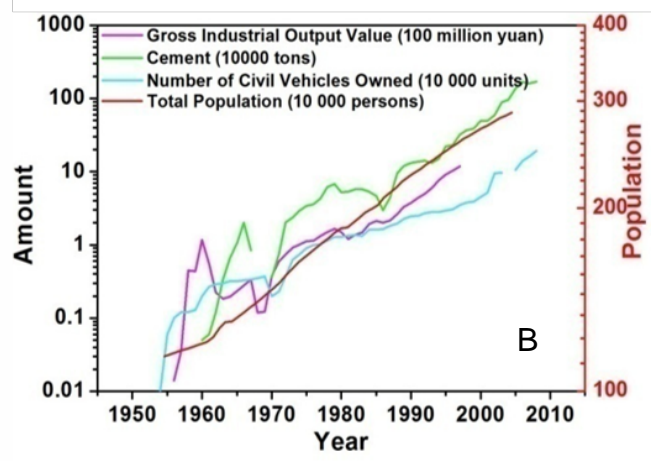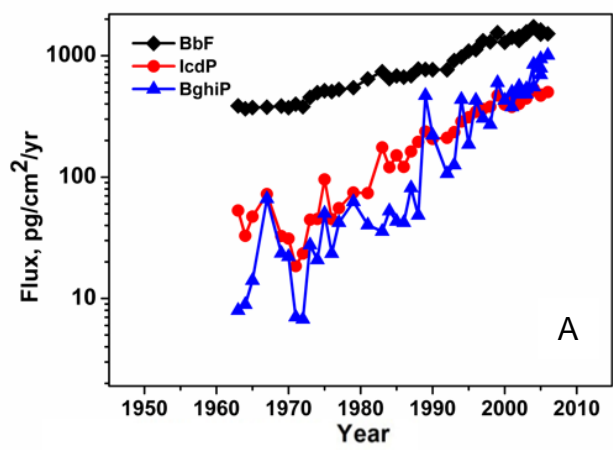
Fig.4 Deposition fluxes of selected PAHs in Lake Cuo Na (A) and population and economic development data of Tibet* (B). *Data from NBSC. China Statistical Yearbook 1949-2008; China Statistics Press, Beijing.

Fig. 5 Bivariate plot of PAH diagnostic ratios in lake sediments.

PAH sources identification by Yunker et al., (2002): FLT/(FLT+PYR) < 0.4: petroleum, 0.4 < FLT/(FLT+PYR) < 0.5: petroleum combustion, FLT/(FLT+PYR) > 0.5: grass, wood and coal combustion; IcdP/(IcdP+BghiP) < 0.2: petroleum, 0.2 <IcdP/(IcdP+BghiP) < 0.5: petroleum combustion, IcdP/(IcdP+BghiP) > 0.5: grass, wood and coal combustion.